

A small muon telescope for high energy gamma-ray astronomy

C.R.A. Augusto¹, C.E. Navia¹, A. Ohsawa², M. Robba¹ and K.H. Tsui¹,

¹*Instituto de Física Universidade Federal Fluminense,
24210-130, Niterói, RJ, Brasil.*

²*Institute for Cosmic Ray Research,
University of Tokyo, Kashiwa, 277-8582 Japan.*

Recebido em 03 de agosto de 2000. Aceito em 10 de maio de 2001.

It is present a progress report on the design and construction of a small muon telescope mounted at sea level as a celestial gamma ray detector, aiming at filling the gap in 30-1000 GeV region between ground-based and satellite-borne instruments. The optimum performance of the telescope is due to its tracking system. In order to provide all the characteristics and the detector sensitivity, a massive Monte Carlo calculation of the muon spectra in the earth's atmosphere has been carried out. The implications of these results in the context of a real possibility of doing gamma-ray astronomy using this telescope are discussed.

I Introduction

Gamma-ray astronomy and cosmic ray physics are closely related topics. Because most of the gamma-rays are formed in processes in which high energy particles take part. By detecting high-energy gamma-rays, it is possible to investigate various objects not only in the Galaxy but far away from it, because practically the whole Galaxy and a significant part of the Metagalaxy are almost transparent to gamma radiation. Gamma-ray astronomy has now become an integrated part of astronomy and astrophysics. The COMPTEL [1] and EGRET [2] experiments have generated the first all-sky gamma source maps up to 30 MeV energy regions. However, there are marked differences between them, because gamma rays have been recorded from several directions in the sky, but not with the same intensity.

Direct measurements of celestial gamma rays have been done using satellite-borne observatories OSSE, COMPTEL, EGRET and BATSE [3]. However, these measurements are limited to energies below ~ 2.0 GeV by the low fluxes and the limited active areas in space. Thus, the gamma-ray astronomy in the very high energy region (above 100 GeV) can be obtained using only indirect methods such as ground-based detectors. However, ground-based detectors can infer information about the nature and energy of primary gammas only from the showers originating from their interactions with air nuclei. This makes such observations extremely dependent on the knowledge of the shower development and propagation in the atmo-

here. Ground-based detectors include detection of: a) the electromagnetic component in air showers (mostly e^\pm), b) the muon contents in the air showers, c) the Cherenkov-light produced by the showers in the atmosphere and d) the detection of deep-underground muons, or a combination of them, while the area sensitive to muons is generally a small fraction ($< 1\%$) of the total air shower array.

Since charged particles cannot go directly from its source to the Earth, because they would be inclined through the Galactic magnetic field, the incoming primary particles from the direction of point sources are neutral and stable particles. So far, there are several experimental evidences that confirm that these neutral particles are gamma-rays. These evidences are in the energy region below 100 GeV [1, 2] obtained by satellite-borne instruments. On the other hand, in the high energy region (above 1 TeV), the ground-based results, based on a number of large arrays, only four sources detected at high significance levels have been confirmed [4, 5, 6] and in most of the cases only the upper limits of the fluxes have been reported.

At sea level, high energy photons from cosmic sources can be detected by means of the muon contents in the showers which they produce in the atmosphere. However, the discrimination of showers produced by gamma-ray from a background of showers produced by cosmic ray (mainly protons) is not easy. In the TeV energy region the number of muons associated with a gamma-ray induced shower is expected on average to be less than 6% of the number expected for a ha-

dron shower. Then muon-poor showers are associated to gamma-rays and this is the main criterion for the selection between gamma and hadron (proton) showers.

In the following sections we give a description of a new small telescope with some especial characteristics. The main goal is to detect muons at sea level, because they are expected as secondary products of the primary interaction of gamma-rays in the atmosphere and our physical motivations are to investigate the existence of new sources in the Southern Hemisphere like:

1. Activity Galactic Nuclei (AGN).
2. Gamma-ray Pulsars.
3. Supernova Remnants.
4. Other possible sources not yet known and the diffuse background radiation.

A large number of different theoretical explanation then appeared concerning the nature of the galactic and extra-galactics sources [7, 8]. Only more solid observational data will decide which of the theories, if any, corresponds to reality. The main goal is to investigate the real possibility of doing gamma-ray astronomy using this telescope and aiming to fill the gap in 30-1000 GeV region between ground-based and satellite-borne instruments, because more experimental data are needed to find its true nature.

II Muon telescope description

An agreement between the High Energy Group of the Universidade Federal Fluminense (UFF) in Brazil and the Institute for Cosmic Ray Research in Japan has been accomplished for the construction of a small muon telescope for joint research. The telescope will be set up in the campus of the UFF Niteroi (Rio de Janeiro State), located at sea level, latitude $22^{\circ} 53' 59'' S$, longitude $43^{\circ} 16' 12'' W$ and mean atmospheric pressure of 1013 mBar. Initially the telescope will operate as a simple storytelling (counter) telescope of muons [9] and the main characteristics are detailed below.

A. Experimental setup

The telescope consists of four identical plastic scintillation counters with $0.5\text{ m} \times 0.5\text{ m}$ of active areas and 0.035 m of thickness, every unit is inside a metallic pyramidal container as is schematized in Fig.1. In the top of the pyramid is placed a square box that sustains a photo-multiplier (PM) Hamamatsu RS521 and a pre-amplifier. When a fast charged particle, for instance a muon, crosses the scintillator, a fluorescent light is emitted by the excited scintillator which is picked up by the PM. The purpose of the photomultiplier is to convert a rather low light intensity into an electrical signal, the signal is pre-amplified to a sufficient amplitude to facilitate further pulse treatment and pulse-height discrimination. In our case, the output signal is

a analogic pulse with a peak around 300 mV. This performance is obtained by using a preamplifier with gain around 70 – 100. Every unit requires very stable power supplies, high voltage ($\sim 1000\text{ V}$) for the PM and low voltage ($\sim \pm 12\text{ V}$) for the preamplifier.

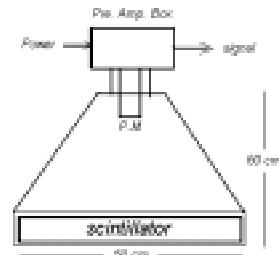


Figure 1. Arrangement of a counter layer, formed by one scintillator inside of a pyramidal box with the photo-multiplier and pre-amplifier units.

The experimentalist's task is to compute the muon intensity in the atmosphere initiated by gamma rays coming from celestial point sources, given the coincidence counting rate of multi-element cylindrically symmetric with squared cross sections. In order to obtain a narrow collimator aperture, the telescope is formed for three squared scintillator counter layers, the top, middle and bottom layers schematized as A, B and C in Fig.2. The gap between layers is 1.5 m. The counter layers are set up in a structure that allows to have two rotation axes. The telescope has also a fourth scintillator, D, put closed with the C scintillator counter. The purpose of this scintillator is to use as a selective trigger. We discuss these aspects with more detail in the section III again.

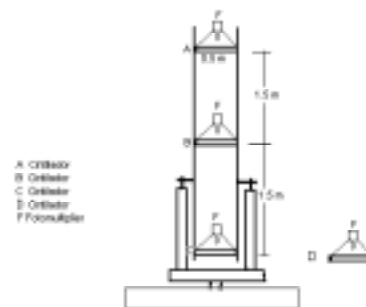


Figure 2. Layout of the muon telescope. The letters A, B, C and D indicate the position of the four counter layers. The telescope has a structure with two rotation axes, zenithal and azimuthal in the horizontal system or declination and right ascension in the equatorial system.

B. Angular resolution

For energies above 1 GeV the muons arrival directions are close with the primary gamma ray direction, in this case the muon produces a coincidence among the A, B and C counter layers. The angular resolution of the telescope is defined by the distance between the A and C scintillation counters (3.0 m) and by the scintillator width (0.5 m). Under these conditions, the opening angle is 9.4 degrees and the associated solid angle is 0.085 sr. The low angular resolution of 9 degrees of the telescope is compensated with a good geometrical factor ($68.2 \text{ cm}^2 \text{ sr}$) and for the servo mechanism that locates and follows the source. These characteristics are essential for gamma-ray astronomy study using a small telescope.

C. Geometrical Factor

The factor of proportionality relating the coincidence counting rate C to the muon intensity I is called the geometrical factor G [10] and can be expressed, when the intensity is isotropic as

$$C = G I, \quad (1)$$

with

$$G = \int_{\Omega} d\omega \int_S d\bar{\sigma} \cdot \bar{r}. \quad (2)$$

Here $d\omega$ is the element of solid angle; Ω is the domain of ω , this is limited by the other telescope sensors; \bar{r} is the unit vector in direction ω ; $d\sigma$ is the element of surface area of the last telescope sensor to be penetrated and $\bar{r} \cdot d\sigma$ is the effective element of area looking into ω . We consider only the case where the detection efficiency for muons, $\epsilon(E)$, depends only on the energy, where I is defined as

$$I = \int_0^{\infty} dE J_0(E) \epsilon(E), \quad (3)$$

where $J_0(E)$ is the spectral intensity of muons ($s^{-1} \text{ cm}^{-1} \text{ sr}^{-1} E^{-1}$). In this approximation, the geometrical factor depends only on the size of the telescope and taking into account the fact of a cylindrically symmetric telescope with three rectangular detectors, the geometrical factor is obtained after integration of the relation (2) as [11]

$$G = L^2 \ln\left(\frac{L^2 + a^2}{L^2 + 2a^2} \times \frac{L^2 + a^2}{L^2}\right) + 4a(L^2 + a^2)^{1/2} \text{tg}^{-1}\left(\frac{a}{(L^2 + a^2)}\right) - 4aL \text{tg}^{-1}\frac{a}{L}. \quad (4)$$

In our telescope $L = 1.5 \text{ m}$ and $a = 50 \text{ cm}$ giving a geometrical factor of $G = 68.2 \text{ cm}^2 \text{ sr}$.

D. Triggering system

There are two trigger modes. The first is hardware trigger, where the coincidence between the signals from

the top, middle and bottom layers are used (see Fig.3). The B scintillator has been put in the telescope only for minimizing the random coincidences. The pulses from the A, B and C detectors come to discriminator block in which they are shaped to 60 ns duration. The choice of this pulse length is determined in order to take into account the difference in the time of flight delay of the muons between the top and bottom telescope layers, estimated in 10 ns. The shaped signals go then to the logic unit which form logical "AND". Under these conditions the output coincidence pulse has a length of 50 ns.

The second mode is a selective trigger, and it is implemented in order to not consider coincidences in the first trigger mode originated by showers initiated for cosmic ray background. It uses another detector, D, which is out of the axis of the telescope. The pulse of this detector is discriminated to 60 ns duration too and is placed in anti-coincidence with the output coincidence of the first trigger mode. This window time is enough to produce a trigger with a resolution time of 20 ns, without use of different cable length to compensate the systematic delay. The Fig.3 and Fig.4 summarize the situation.

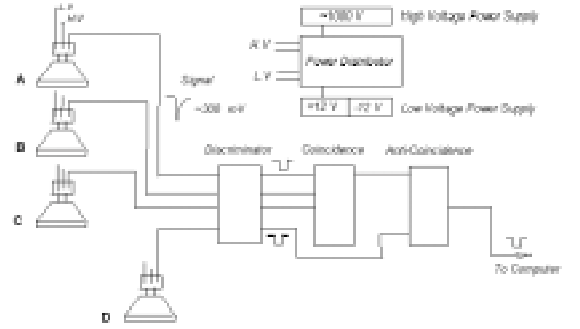


Figure 3. The two trigger modes used for the muon counting rate, around the source direction.

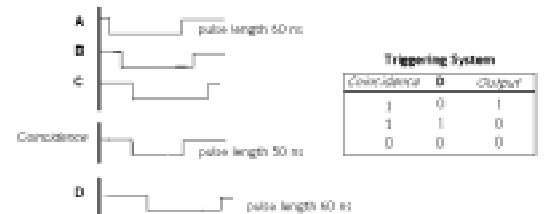


Figure 4. Discriminator output pulses from A, B and C detectors, showing the retard of the pulses, before and after the coincidence (hardware trigger), as well as before and after the anti-coincidence (selective trigger).

E. Tracking system

The principal disadvantage of a small muon telescope is its small active area. This limitation places a cutoff in the primary gamma energy observed by the telescope, or in other words, it is possible to detect primary gamma-rays only with energies below 10^{14} eV, because the primary gamma-ray flux decreases when the energy increases. However, a small muon telescope can be set up as an optical telescope controlled by a computer to locate and follow a certain gamma-ray point source. In this case, the muon background to be considered (produced by conventional cosmic ray particles) is only inside the small solid angle, always around the source direction. When the telescope is mounted in an equatorial system, it is easy to follow a celestial object of interest, using a motor to rotate the telescope about the polar axis and to compensate the apparent rotation of the heaven due the Earth's rotation. This is done with the present muon telescope here described.

F. Data acquisition system

The data acquisition system is based on a PC computer, where commands for the measurement actions are concentrated. There are two independent units connected as peripheral ones to the PC expansions bus. The first is a dedicated board linked to the telescope output. A resident programme (Lab-View) takes the control of the coincidence counting rate process during the continuous operation. The read-out time of each event is around 32 microseconds. Another variables like the sidereal time and declination are registered too.

The second is a dedicated board too, for the servo mechanism control. This mechanism is formed by two step motors linked to declination and right ascension. They are controled for an another resident programme Scope. The source code of the Scope program was written in C language, it is a free software and can be obtained from the web by download [12].

III Background

In order to set the scale of the fluxes of cosmic photon beams from point sources and other sources, like the diffuse γ -ray flux, only the most relevant prediction of diffuse gamma ray fluxes in the energy region of 10^{12} to 10^{15} eV is take into account. On the other hand, to obtain the main background, or in other words the number of muons from cosmic ray (mainly protons) showers in the same direction of the photon beam from point sources, as is expected in the telescope, we performed a massive Monte Carlo calculation.

A. Diffuse γ -ray flux

Figure 5 shows the predictions for the fluxes of galactic and extra-galactic diffuse cosmic photons. The total cosmic ray flux and the primary electron flux are shown for comparison. The origin of the galactic diffuse cosmic photons is not very well established yet. However, it is very probably that they are a consequence of the interaction of cosmic ray particles (in the PeV energy region) with interstellar gas in the galactic disk, through the process

$$p + p = \pi^0 + X, \quad (5)$$

and followed by $\pi^0 \rightarrow 2\gamma$. The theoretical prediction [13, 14] of galactic diffuse γ -flux is shown in Fig.3 as the ISM flux. The ratio between this diffuse γ -ray flux and the cosmic ray flux is estimate as

$$\frac{I_\gamma}{I_{CR}} \sim 8 \times 10^{-5}. \quad (6)$$

On the other hand, the extra-galactic diffuse cosmic photons are expected as a consequence of the interaction of the extra-galactic cosmic ray with the 3 K background photons, through the process

$$p + 3K\text{photon} = \pi^0 + X, \quad (7)$$

and followed by $\pi^0 \rightarrow 2\gamma$. The proton energy threshold for this process is near 10^{20} eV, because in the rest proton system the 3 K photons are gamma rays. The prediction for this diffuse gamma flux is shown also in Fig.3 [15] and the ratio is expected as

$$\frac{I_\gamma}{I_{CR}} \sim 1.0 \times 10^{-5}. \quad (8)$$

As the muon content in γ showers is around only 5% of the muon content in proton showers, the number of muons from diffuse (galactic and extra galactic) γ -ray flux expected in the same solid angle sustained by the telescope is around 5×10^{-7} smaller than the number the muons from cosmic ray flux, consequently they can be ignored. On the other hand, the contribution of the diffuse electronic flux to the muon noise in the telescope is around 10^{-5} times smaller than the number the muons from cosmic ray flux, consequently it is ignored too.

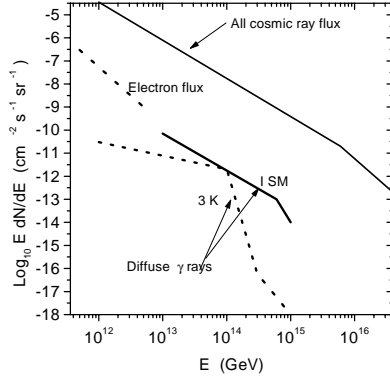


Figure 5. Galactic and Extra galactic diffuse cosmic photons predictions. The total cosmic ray flux and the primary electron flux are shown for comparison.

B. Diffuse cosmic rays flux

The present study is devoted to the muon flux in the atmosphere, produced by diffuse cosmic rays flux (see Fig.5). In ground-based detectors, these muons constitute the main background in the gamma-rays detection from celestial point sources. The integral energy spectrum of the cosmic ray flux in the TeV energy region is obtained after the integration of the differential flux represented by the bold line in Fig.5, and is given by

$$\phi_{CR}(> E_0) = 3.3 \cdot 10^{-7} ;$$

$$(E_0/10TeV)^{-1.7} \text{ cm}^{-2} \text{ s}^{-1} \text{ sr}^{-1}. \quad (9)$$

The calculations of the muon spectra in the Earth's atmosphere produced by these cosmic rays have been carried out on the basis of the COLLI [16] Monte Carlo generator of hadron-hadron, hadron-nucleus and nucleus-nucleus interaction in a wide range of energies. The COLLI is based in the quark-string model (QGSM), also known as dual parton model. Some simulation input used for atmospheric propagation, as well as for the photo production study is shown in Appendix A.

After the generation of 10,000 events, the differential energy spectra of muons for several zenithal angles and at sea level are shown in Fig.6. We can see that the large atmospheric thickness existent at large zenith angles (see Appendix A) makes the atmosphere opaque for muons of low energy. This characteristic is seen again in Fig.7, where the dependence of the integral energy spectra of muons with the zenith angle are shown.

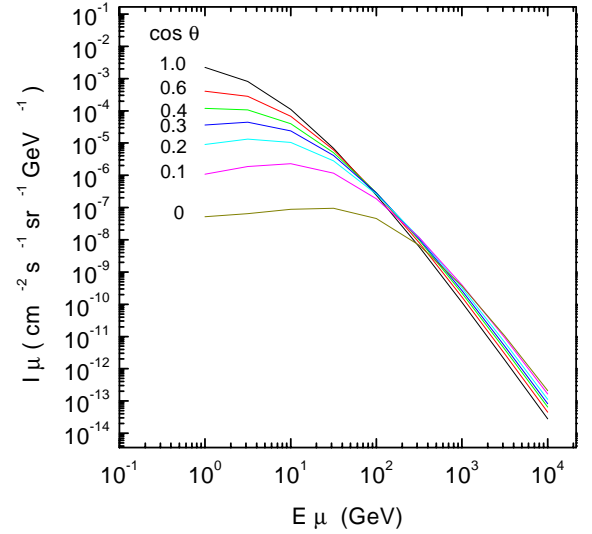


Figure 6. Differential energy spectra of muons (background) at sea level and for several zenith angles.

IV Signal to noise ratio

In order to obtain the signal to noise ratio of a source tracking telescope of muons, used as celestial detector of gamma-rays, we would like to make the following considerations:

a) The signal is the muon content of showers generated by gamma-rays along the declination and right ascension of the source. We admit that the gamma rays flux from a source has an integral energy spectrum as $J_\gamma(> E) = J_\gamma^0 E^{-\beta}$ and the number of muons in the telescope, associated with the source is given by

$$N_\mu(\text{signal}) = J_\gamma(> E) A N_\mu^\gamma t. \quad (10)$$

Here, A is the active area of the scintillators (2500cm^2), t is the exposure time (on-source) and N_μ^γ is the number of muons per gamma ray shower. This last quantity is very hard to be obtained by an analytical calculation, because it has a zenith angle and muon threshold dependence and here it is obtained by a Monte Carlo calculation.

b) The main noise is generated by the muon contents of showers initiated by primary cosmic ray

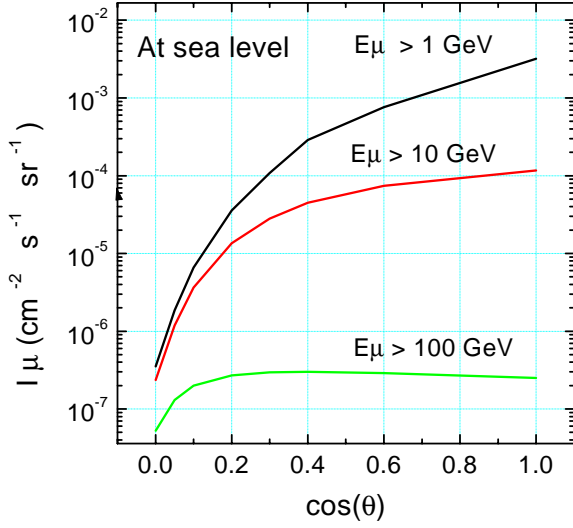


Figure 7. Dependence of the integral energy spectra of muons (background) with the zenith angle.

(mainly protons). Even so, primary charged particles are produced by diffuse sources and they are almost injected isotropically in the upper atmosphere with an integral energy spectrum such as $J_{CR}(> E_0) = 3.3 \cdot 10^{-7} (E_0/10TeV)^{-1.7} cm^{-2} s^{-1} sr^{-1}$. Then, the muon flux $J_\mu(> E_\mu, \cos\theta)$ is obtained at sea level from a Monte Carlo calculation (see Fig.5) for several zenith angles. Under these considerations, the background counting rate of the muons expected in the telescope is calculated as

$$R(> E_\mu, \cos\theta) = J_\mu(> E_\mu, \cos\theta) G, \quad (11)$$

where G is the geometrical factor of the telescope with $G = 68.2 cm^2 sr$ (see section II, B). Figure 8 shows the zenith angle dependence of the rate for several muon threshold energies. The effective number of background muons expected in the same solid angle around the zenith angle (θ) is determined by

$$N_\mu(> E_\mu, \cos\theta) = R(> E_\mu, \cos\theta) t, \quad (12)$$

where t is the exposure time.

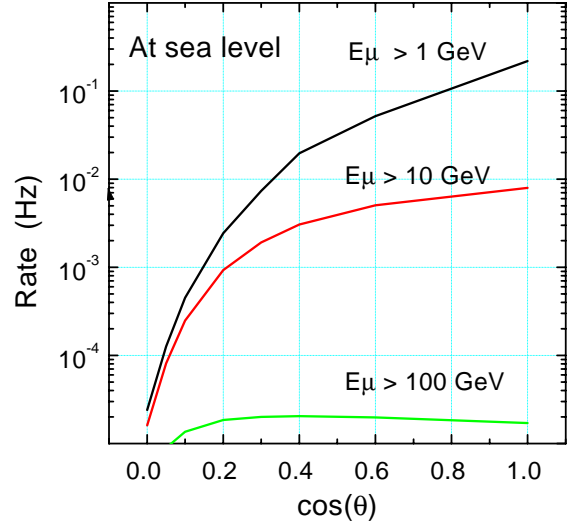


Figure 8. Dependence of the counting rate of the muons (background) in the telescope with the zenith angle.

c) The signal to noise ratio (S/N) can be obtained as

$$\frac{S}{N} = \frac{N_\mu(\text{signal})}{\sqrt{N_\mu(\text{background})}}. \quad (13)$$

The above expression means that the S/N is proportional to \sqrt{t} .

An analytical expression to the signal to noise ratio is very hard to obtain, and a Monte Carlo is inevitable. Fig.9 and Fig.10 show the exposure time (on-source) of the telescope to reach the required sensibility ($S/N > 1$) to detect some sources, already known [17], such as:

a) 2.5 hours for AGN sources like the Mrk 421 (flux of $\sim 1.5 \times 10^{-6} cm^{-2} s^{-1}$ for $E_\gamma > 10 GeV$).

b) 23 days for sources like the Crab Nebula (flux of $3.0 \times 10^{-7} cm^{-2} s^{-1}$ for $E_\gamma > 10 GeV$).

c) 38 months for sources like the supernova remnant γ Cygni (flux of $3.2 \times 10^{-8} cm^{-2} s^{-1}$ for $E_\gamma > 10 GeV$).

These Monte Carlo calculations of the signal to noise ratio are for a statistical significance level above 3σ .

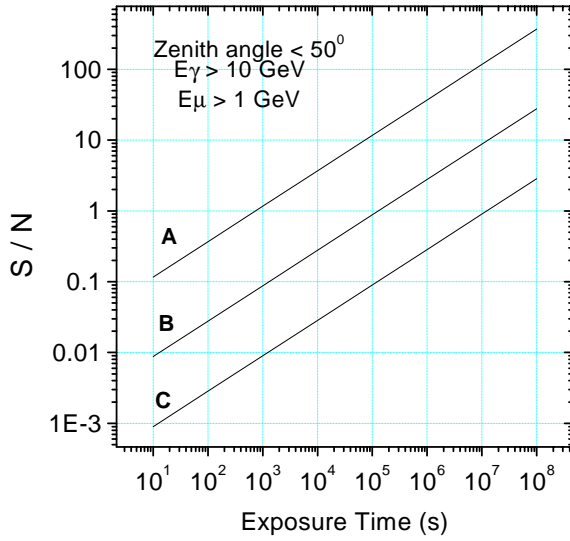


Figure 9. The signal to noise ratio as a function of the exposure time (on-source) for: A AGN sources like the (Mrk 421), B sources like the Crab Nebula and C sources like supernova remnant (γ Cygni). It is considered as sources near to vertical.

V Discussions and conclusions

The expected performances of a small telescope as a celestial gamma-ray detector have been studied. The geometrical factor and directional response of the telescope made of multi-element cylindrically symmetric with squared cross section are presented. The telescope computes the muon intensity given the coincidence counting rate. The important feature of the proposed muon telescope is the source tracking system.

Some specifications are:

Geometrical factor - $68.2 \text{ cm}^2 \text{ sr}$

Active solid angle - 0.085 sr

Range of zenith angle - $0 \text{ to } \pi/2$

Range of azimuthal angle - $0 \text{ to } 2\pi$

Muon registration efficiency - 95%

Tracking system with equatorial mount

Operation time - 24 hours/day (over all year)

Location depth - See level (Niteroi)

This small ground-based gamma-ray detector can explore the energy region between 10 and 1000 GeV.

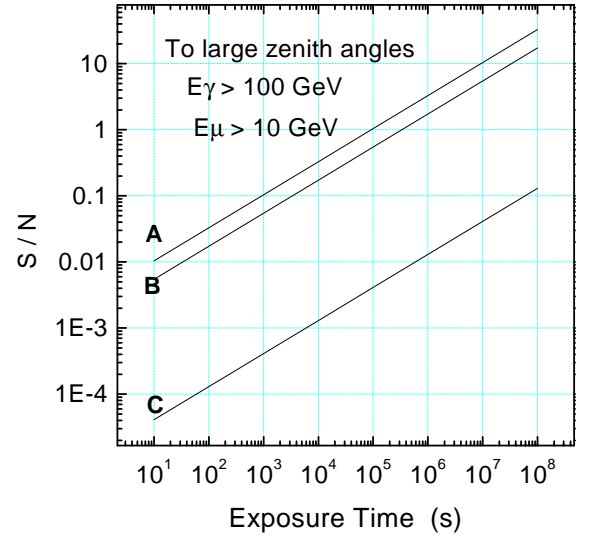


Figure 10. The same than Figure 7. However, it is considered the sources near to horizon.

This region is unexplored for both satellite-borne and ground-based experiments. We would like to search this region, because there is the probability of the existence of new sources not present in other wavelength. Also, it is possible to make the connection between observations made at low energies (satellites) and observations made at high energies (ground-based).

The atmospheric muon background have been obtained from a Monte Carlo Calculation and the signal to noise ratio (S/N) has been determined. Muon excess with a statistical significance level above 3σ from celestial gamma sources with flux around 10^{-6} to $10^{-8} \text{ cm}^{-2}\text{s}^{-1}$ can be obtained under few hours and several month respectively of exposition time. These results show that there is a real possibility of doing gamma-ray astronomy using this telescope and the main objective is to find new sources only accessible in Southern Hemisphere, where the number of ground-based detectors is small.

The above considerations are for a telescope only as a muon counter. However, it is possible to include a magnet spectrometer to measure the momentum and

the charge of incident muon. This stage is of vital importance, since through the spectrum of energy of the muons, it is possible to estimate the energy of the primary gamma that originated them. After a period of tests and some measurements with the counter telescope, this calorimeter will be implanted.

Acknowledgments

The authors wish to express their gratitude to Prof. C. M. G. Lattes, for his encouragement. We are also grateful to Prof. N. Ohmori from Kochi University for his contribution at the early stage of this experiment. This work is partially supported by FAPERJ (Rio de Janeiro State Agency) and for The Institute for Cosmic Ray Research of Tokyo University.

References

- [1] V. Schonfelder et al., *Annals of the New York Academy of Sciences*, Vol.759, Art.21, pp. 226 (The New York Academy of Sciences, New York) 1995.
- [2] G. Kanbach, *MPE Annual Report 1993*. S. 23 (1994).
- [3] V. Shconfelder, *Il Nuovo Cimento*. Vol.19C, N.6, 805 (1996).
- [4] T. C. Weekes et al., *Astrophys J.* **342**, 379 (1989).
- [5] M. Punch et al., *Nature* **358**, 477 (1992).
- [6] T. Kifune et al., *Astrophys J. Lett.* **438**, L92 (1995).
- [7] T. C. Weekes, *Phys. Rep.* **160**, 1 (1988).
- [8] T. K. Gaisser, *Science* **247**, 1049 (1990).
- [9] Y. Yamashita et al., *Nucl. Inst. and Meth. A* **374**, 245 (1996).
- [10] J. D. Sullivan, *Nucl. Inst. and Meth.* **95**, 5 (1971).
- [11] A. Velarde, Graduate Thesis, UMSA La Paz (1979)(Unpublished).
- [12] <http://www.zebu.uoregon.edu>.
- [13] V. S. Berezinsky et al., *Sov. Astron. Lett.* **14**, 847 (1988).
- [14] F. Halzen et al., *Phys. Rev. D* **41**, 342 (1990).
- [15] M. T. Ressel et al., *Comment Astrophys* **14**, 323 (1990).
- [16] N. S. Amelin et al., *Sov.J. Nucl. Phys.* **51**, 1 (1990).
- [17] V. G. Sinitsyna., *Il NUovo Cimento* Vol. **19C**, N6, 965 (1996).
- [18] P. Lipari, *Astroparticle Phys.* **1**, 195 (1993).
- [19] T. Ahmed et al., H1 Collaboration, *Phys. Lett. B* **299**, 374 (1993).
- [20] M. Drees and K. Grassie., *Z. Phys. C* **28**, 451 (1985).

VI Appendix. Some simulation inputs

A. Atmospheric model

Under the supposition that the atmosphere is a perfect gas in hydrostatic equilibrium [18], the atmospheric depth X can be related with the height h on sea level as

$$X(h) = \begin{cases} X_0 \exp(-h/h_0), & \text{if } h \geq 11 \text{ km}; \\ A(h_b - h)^{\alpha-1}, & \text{if } h \leq 11 \text{ km} \end{cases} \quad (14)$$

When km is used to measure h and g/cm^2 to measure X , the constants are $A = 2.303 \times 10^{-6}$, $h_0 = 6.344$, $h_b = 44.33$ and $\alpha = 4.253$.

For large zenith angles, we need to take into account the curvature of the Earth. The correlation between the atmospheric depth and the zenith angle it is shown in Fig.11.

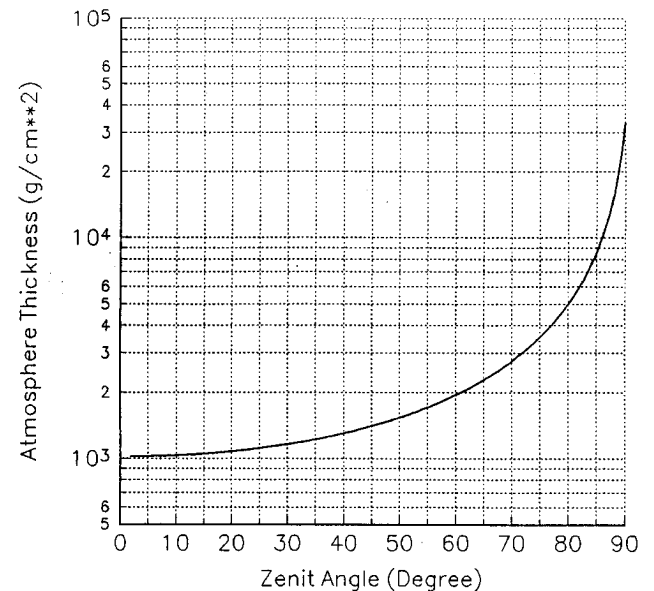


Figure 11. Correlation between the atmospheric depth and the zenith angle.

B. Photoproduction

After Kiel group announced the discovery of a large flux of γ -rays of high energy ($\sim 10^{15}$ eV) from Cygnus X-3, with large muon contents, not confirmed today by large arrays, many groups have claimed an anomalous increase of the cross section of photo production with the energy of the γ -ray, as a consequence of such high energy, the structure of a photon should be very close of the structure of a gluon.

Even so, recently the photo production was studied in detail at HERA in the energy region of 194 GeV in the c.m. system [19], using the interaction of quasi-real photons γ^* in the reaction $ep \rightarrow e' + \gamma^*p \rightarrow e' + x$. The

total cross section of photo production was established as

$$\sigma_{total}(\gamma p) = 156 \pm 18 \text{ } \mu b. \quad (15)$$

This value agrees well with a normal extrapolation of the data in the area of low energy and not with theoretical predictions that foresee an anomalous increase [20].

On the other hand, the values for the partial photo production cross section ratios, were found as

$$\sigma_{nd}(\gamma p)/\sigma_{total} = 0.66, \text{ Inelastic nondiffractive,} \quad (16)$$

$$\sigma_d(\gamma p)/\sigma_{total} = 0.23, \text{ Inelastic diffractive,} \quad (17)$$

$$\sigma_{el}(\gamma p)/\sigma_{total} = 0.11, \text{ elastic.} \quad (18)$$

The change of the cross section of photo production with the mass of the target nucleus can be described by

$$\sigma(\gamma A) = A^\delta \sigma(\gamma p), \quad (19)$$

where A is the atomic number of the target nucleus, $A = 14.4$ for air. usually δ is determined using experimental data for two or more different nuclei. Even so, unfortunately, there are no precise data and we adopted $\delta = 0.91$ in the practical calculations. The inelastic cross section is connected with the collision mean free path λ_{coll} by

$$\lambda_{coll} = \frac{A}{N\sigma(\gamma A)}, \quad (20)$$

where N is Avogadro's number.